# Extending Wertheim's perturbation theory to the solid phase of Lennard-Jones chains: Determination of the global phase diagram

C. Vega
*Departamento de Química Física, Facultad de Ciencias Químicas, Universidad Complutense, 28040 Madrid, Spain*

F. J. Blas
*Departamento de Física Aplicada, Escuela Politécnica Superior, Universidad de Huelva, 21819 La Rábida, Huelva, Spain*

A. Galindo
*Department of Chemical Engineering and Chemical Technology, Imperial College of Science, Technology and Medicine, Prince Consort Road, London SW7 2BY, United Kingdom*

(Received 6 November 2001; accepted 6 February 2002)

Wertheim's first order thermodynamic perturbation theory (TPT1) [M. S. Wertheim, J. Chem. Phys. **87**, 7323 (1987)] is extended to model the solid phase of chains whose monomers interact via a Lennard-Jones potential. Such an extension requires the free energy and contact values of the radial distribution function for the Lennard-Jones reference system in the solid phase. Computer simulations have been performed to determine the structural properties of the monomer Lennard-Jones system in the solid phase for a broad range of temperatures and densities. Computer simulations of dimer Lennard-Jones molecules in the solid phase have also been carried out. The theoretical results for the equation of state, the internal energy, and the sublimation curve of the dimer model in the solid phase are in excellent agreement with the simulation data. The extended theory is used to determine the global (solid–liquid–vapor) phase diagram of the LJ dimer model; the theoretical estimate of the triple point temperature for the LJ dimer is $T^*=0.653$. Similarly, Wertheim's TPT1 is used to determine the global phase diagram of chains formed by up to 8 monomer units. It is found that the calculated triple point temperature is hardly affected by the chain length, and that for large chain lengths the fluid–solid equilibrium coexistence densities are virtually independent of the number of monomers in the chain when the densities are expressed in monomer units. This is in agreement with experimental indications observed in polyethylene, where both the critical and the triple point temperatures tend to finite values for large molecular weights. © *2002 American Institute of Physics.* [DOI: 10.1063/1.1465397]

## I. INTRODUCTION

In the mid-1980s Wertheim presented a very successful theory to study the thermodynamic properties of hard-core fluids interacting via short-range attractive (association) forces,[1–4] such as hydrogen bonding fluids. In this model, when the association strength becomes infinitely strong chains are formed from a fluid of associating monomers.[5] In this way it is possible to derive an equation of state for a chain of freely-jointed tangent hard segments using only thermodynamic information of the monomer reference fluid. In the simplest implementation of the theory, which is commonly denoted as the first order thermodynamic perturbation theory (TPT1), the only information required in order to build an approximate equation of state for the chain fluid is the equation of state of the monomer fluid and its pair correlation function at contact. The equation of state (EOS) arising from TPT1 was proposed independently by Wertheim[6] and by Chapman, Jackson, and Gubbins.[7] In the early 1990s Chapman[8] showed that Wertheim's formalism could also be applied to systems with attractive (dispersion) forces. The work of Johnson *et al.*[9,10] has shown that Wertheim's formalism yields a good description of the Lennard-Jones (LJ) chain fluid, provided that the EOS and pair correlation function of the reference LJ fluid are accurately known. The same is true for chains formed from monomers interacting via other pair potentials, for instance, the square well potential[11] and the Yukawa potential[12] have also been incorporated in this context. Therefore, an approximate but reliable description of the fluid phase of fully flexible chains (i.e., with no constraint in the bonding angle or torsional state) can be obtained nowadays in a rather straightforward way. The TPT1 theory of Wertheim provides reasonable predictions of the vapor–liquid equilibria for a number of different types of chain.[13–16] Notice that other theoretical treatments are also succesfull for LJ chains.[17]

In order to obtain the global phase diagram of flexible chains, the solid phase should also be considered so that fluid–solid coexistence is adequately located within the phase diagram of the model. In the last decade the fluid–solid equilibrium of a number of molecular models have been considered, for example, hard dumbbells, quadrupolar hard dumbbells, hard spherocylinders, hard ionic systems, benzenelike models, and others (see, for instance, the recent review of Monson and Kofke[18]). However, efforts consider-

 

ing the fluid–solid equilibrium of flexible chains are scarce. Malanoski and Monson[19] have determined via computer simulation the fluid–solid equilibrium of freely jointed hard sphere chains, and of a hard model of *n*-alkane molecules.[20] Polson and Frenkel[21] have determined the fluid–solid equilibria of LJ chains (with a bending potential) and of a LJ model of *n*-alkane molecules.[22] Theoretical works describing the phase equilibria of flexible chains in the solid phase are even more scarce, the work of Sear and Jackson,[23] and of Malanoski *et al.*,[24] in which the the cell theory is extended to study the solid phase of these molecules, are the exception.

Solid phases of long flexible molecules are of interest since it is at room temperature and pressure that these molecules exhibit the solid phase. For instance, all linear alkanes with more than 20 carbon atoms are solids at room temperature and pressure, and the same is true for polyethylene.[25] In many industrial processes one has to deal with the fluid–solid separation of alkane mixtures. A theoretical description of the solid phase of flexible chain molecules would be of great interest both from a fundamental and from a practical point of view. Taking into account the success of Wertheim's TPT1 approach in modelling the fluid phase of chain molecules one is tempted to raise the following question: can the approach be extended to describe the solid phase of flexible chains? Recently Vega and MacDowell[26] have shown that Wertheim's TPT1 can be extended to the solid phase of freely jointed hard spheres obtaining excellent agreement with the simulation results of Malanoski and Monson.[19] The theory is also able to describe the solid phase of two-dimensional freely jointed discs.[27] Although chains formed by hard spheres are of interest, it would certainly be more interesting to consider the case of chains formed by Lennard-Jones monomers. Due to the presence of attractive forces, the Lennard-Jones model exhibits vapor–liquid equilibria in addition to the fluid–solid equilibrium, and is therefore of greater practical interest. The goal of this paper is to extend Wertheim's theory to the solid phase of freely jointed LJ molecules and to provide a first estimate of the global phase diagram of these systems.

Let us briefly discuss the solid structure of freely-jointed chains. In a freely jointed chain there is neither bending nor torsional potentials between the monomers of the chain (although there is an intramolecular pair interaction between monomers of the same chain separated by more than one bond). Therefore there is no energetic penalty when the atoms of the chains adopt a close-packed structure (for instance the face centered cubic fcc close-packed structure) with an ordered arrangement of atoms but with no long-range orientational order in the bond vectors of the chains. Wojciechowski *et al.*[28,29] were the first to realize this important feature in a continuum hard two-dimensional model. In fact Wojciechowski *et al.*[28,29] showed that the stable solid structure of tangent hard-disc dimers in two dimensions is formed by a close-packed arrangement of atoms with a disordered arrangement of bonds. The same idea holds for hard chains in three dimensions,[19] and one may expect that the same would occur for a three-dimensional LJ chain. In a sense this is a clever solution of nature. The molecules achieve the close-packed structure of hard spheres, so that the density is high, and the system is ordered from the point of view of the atoms but not from the point of view of the molecular bonds. The disorder of bonds means that there is an additional contribution to the entropy of the system arising from the degeneracy of the structure. For this reason the stable solid structure for freely jointed models is one with disordered bonds. The extreme flexibility of freely jointed models makes the existence of such a solid possible. Any reduction of flexibility, such as fixing a bond angle in the model, would make the existence of the closed-packed solid with random bonds impossible, since it is likely that the molecular bonding angle would not be compatible with the angles of an fcc arrangement of atoms. As discussed earlier, in the TPT1 approximation a freely-jointed chain is assumed, hence, the expected structure of its solid phase corresponds to that with the monomer segments arranged in an fcc lattice with random bond orientations. Assuming this structure we have used computer simulations to compare with the theoretical calculations.

The scheme of this paper is as follows: In Sec. II the extension of Wertheim's theory to the solid phase of LJ chains is described. In Sec. III details of the simulations performed in this work are given. In Sec. IV the results for the LJ dimer system are presented, and in Sec. V the global phase diagrams of LJ chains are presented.

## II. BRIEF DESCRIPTION OF WERTHEIM'S PERTURBATION THEORY

We summarize the main ideas contained within Wertheim's theory by following the formulation introduced by Zhou and Stell.[30–32] Let us assume that we have a certain number, $N^{\mathrm{ref}}$, of spherical monomer particles within a certain volume $V$ at temperature $T$, and that these particles interact through a spherical pair potential $u^{\mathrm{ref}}(r)$. In this work the pair potential $u^{\mathrm{ref}}(r)$ is the Lennard-Jones potential with parameters $\sigma$ and $\epsilon$. We denote this fluid as the reference fluid and the properties of this reference fluid will be labeled by the superscript ref. Let us also assume that in another container of volume $V$ and temperature $T$, we have $N=N^{\mathrm{ref}}/m$ fully flexible chains of $m$ monomers each. By fully flexible chains we mean chains of $m$ monomers, with a fixed bond length of $L=\sigma$, and no other constraints (i.e., there is no restriction in either bonding angles or in torsional angles). Each monomer of a certain chain interacts with all the other monomers in the system (i.e., in the same molecule or in other molecules with the only exception of the monomer/s to which it is bonded) with the pair potential $u^{\mathrm{ref}}(r)$. The chain system described so far will be denoted as the chain fluid.

The Helmholtz free energy of the reference fluid $A^{\mathrm{ref}}$ can be divided into an ideal and a residual part as

$$\frac{A^{\mathrm{ref}}}{N^{\mathrm{ref}}kT}=\frac{A^{\mathrm{ref}}_{\mathrm{ideal}}}{N^{\mathrm{ref}}kT}+\frac{A^{\mathrm{ref}}_{\mathrm{residual}}}{N^{\mathrm{ref}}kT}=\ln(\rho^{\mathrm{ref}})-1+\frac{A^{\mathrm{ref}}_{\mathrm{residual}}}{N^{\mathrm{ref}}kT}, \quad (1)$$

where $\rho^{\mathrm{ref}}$ is the reduced number density of the reference fluid ($\rho^{\mathrm{ref}}=N^{\mathrm{ref}}\sigma^3/V$). In Eq. (1) we have arbitrarily assigned the value of thermal de Broglie wavelength to be $\sigma$. The residual term represents the difference between the ref-

erence fluid and that of a system without intermolecular interactions at the same temperature and density.

The free energy of the chain fluid $A$ can also be divided into an ideal and a residual part, so that

$$\frac{A}{NkT}=\frac{A_{\text{ideal}}}{NkT}+\frac{A_{\text{residual}}}{NkT}=\ln(\rho)-1+\frac{A_{\text{residual}}}{NkT}, \tag{2}$$

where $\rho$ is the reduced number density of chains (i.e., $\rho=N\sigma^3/V$). Note that the thermodynamic properties without the superscript ref refer to the chain fluid. In addition to the reduced number density of chains, the reduced number density of monomers in the chain fluid $\rho_m$ is defined as $\rho_m=mN\sigma^3/V$. This density is useful when comparing the properties of chains of different lengths since it seems more appropriate to compare them at the same reduced number density of monomers. Following Zhou and Stell, the residual properties of the chain fluid are given, after several approximations, as

$$\frac{A_{\text{residual}}}{NkT}=m\frac{A^{\text{ref}}_{\text{residual}}}{N^{\text{ref}}kT}-(m-1)\ln y^{\text{ref}}(\sigma), \tag{3}$$

where $y^{\text{ref}}(\sigma)$ is the background correlation function[33] of the reference (monomer) fluid at contact length. The background correlation function is related to the pair correlation function $g^{\text{ref}}(r)$ by

$$y^{\text{ref}}(r)=\exp(\beta u^{\text{ref}}(r))g^{\text{ref}}(r), \tag{4}$$

where $\beta=1/(kT)$. Since for the LJ potential $u^{\text{ref}}(\sigma)=0$, it holds that $y^{\text{ref}}(\sigma)=g^{\text{ref}}(\sigma)$. Therefore, the free energy of the chain fluid can be written as

$$\frac{A}{NkT}=\ln(\rho)-1+m\frac{A^{\text{ref}}_{\text{residual}}}{N^{\text{ref}}kT}-(m-1)\ln g^{\text{ref}}(\sigma). \tag{5}$$

The above equation shows that the free energy of the chain fluid may be obtained from a knowledge of the residual free energy of the reference fluid and the pair background correlation function of the reference fluid at the bonding distance of the monomers in the chain. The equation of state which follows from Eq. (5) is given by

$$Z=mZ^{\text{ref}}-(m-1)\left(1+\rho^{\text{ref}}\frac{\partial \ln g^{\text{ref}}(\sigma)}{\partial \rho^{\text{ref}}}\right), \tag{6}$$

where we have defined $Z^{\text{ref}}$ as $Z^{\text{ref}}=p^{\text{ref}}/(\rho^{\text{ref}}kT)$. The residual part of the internal energy $U$ is given by

$$\frac{U}{NkT}=m\frac{U^{\text{ref}}}{N^{\text{ref}}kT}+(m-1)T\left(\frac{\partial \ln g^{\text{ref}}(\sigma)}{\partial T}\right). \tag{7}$$

We denote Eqs. (5), (6), and (7) as Wertheim's TPT1 theory, noting that the arguments used to arrive to Eqs. (5), (6), and (7) make no special mention as to the actual nature (i.e., fluid or solid) of the phase considered.[30,32] We suggest the use of these two equations for *both* the fluid phase and the solid phase. All that is then needed in order to obtain a unified theory for the phase equilibria of chain molecules is the residual free energy, compressibility factor and pair correlation function of the monomer system both in the fluid and the solid phase. Johnson *et al.*[9,10] have provided values of the free energy, and the structural properties [i.e., $g^{\text{ref}}_{\text{fluid}}(\sigma)$] of the monomer LJ fluid. In this work we use their implementation of the TPT1 approach[9,10] in what relates to the fluid phases. Van der Hoef[34] has recently proposed an analytical expression for the free energy of the LJ monomer solid. His analytical expression is essentially a fit to the most recent simulation results for the solid phase of this model. We adopt the expression provided by van der Hoef for the free energy of the LJ monomer solid. The other information required by the theory is the value of $g^{\text{ref}}_{\text{solid}}(\sigma)$ for the LJ monomer solid. Since this is not available from previous works we have performed computer simulations of the LJ monomer system in the solid phase in order to obtain $g^{\text{ref}}_{\text{solid}}(\sigma)$ for a number of temperatures and densities. The simulation results of $g^{\text{ref}}_{\text{solid}}(\sigma)$ were fitted to an empirical expression of the same form as that proposed by Johnson *et al.* for the fluid phase.[10] In order to check the theory we have also performed a number of computer simulations of the LJ dimer system in the solid phase. Details of the simulations are given in the following section.

## III. SIMULATION DETAILS

### A. Computer simulations of the LJ monomer in the solid phase

We have used the canonical ensemble ($NVT$) Monte Carlo (MC) simulation technique to obtain the pair radial distribution function at contact length in a system of Lennard-Jones spheres in the solid phase. All simulations were carried out for $N^{\text{ref}}=500$ particles, with initial configurations of particles arranged in cubic close packing. In particular, the Lennard-Jones spheres are arranged on a face-centered cubic or fcc structure.

As corresponds to an $NVT$ Monte Carlo simulation, the number of particles, volume, and temperature are specified *a priori*, allowing the pressure and internal energy to fluctuate. Attempts to displace a molecule in a random manner are made in order to reach internal equilibrium. Periodic boundary conditions and the minimum image convention are also used. The calculation of the configurational internal energy is performed in the usual way by truncating the Lennard-Jones interactions at a distance $r_c=3\sigma$, and the pressure is obtained using the virial equation.[35] The total internal configurational energy and pressure are recovered by adding back the standard long-range corrections. The pair radial distribution function is calculated using the standard procedure[35] with a grid space $\Delta r=0.01\sigma$. Such a fine grid is required since $g^{\text{ref}}_{\text{solid}}(\sigma)$ changes significantly in the proximities of $\sigma$, and this effect is especially important in the solid phase. The total simulation length is set to 200 000 cycles, with 50 000 equilibration cycles and 150 000 averaging cycles. Each cycle consists of $N^{\text{ref}}$ attempted particle displacements. The errors are estimated by dividing the simulation in blocks of 10 000 cycles, so as to obtain statistically-independent block sequences, and calculating the standard errors of the mean.

The results obtained in this work are expressed in terms of reduced units, so that $\sigma$, the diameter in the Lennard-Jones potential, is the unit of length, and the maximum attractive energy $\epsilon$ of the potential is the energy unit. The reduced temperature and pressure are defined as $T^*=kT/\epsilon$ and $p^*$

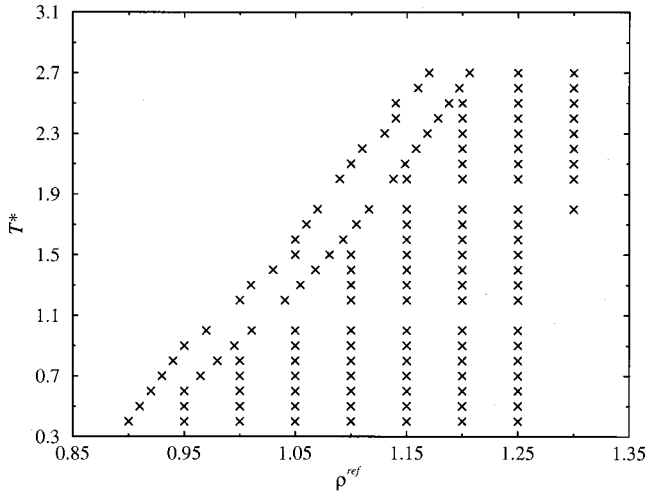


FIG. 1. States for which *NVT* simulations of the LJ monomer solid were performed. For each state the value of $g^{\mathrm{ref}}_{\mathrm{solid}}(\sigma)$ was obtained.

$=p\sigma^3/\epsilon$. In the Lennard-Jones (LJ) monomer reference fluid the reduced number density is denoted $\rho^{\mathrm{ref}}$ (we suppress the superscript $*$ in order to keep the notation as simple as possible), and it is defined as $\rho^{\mathrm{ref}}=N^{\mathrm{ref}}\sigma^3/V$.

We have considered 134 state-points building up a $T^*\rho^{\mathrm{ref}}$ grid in which the radial distribution function of the solid Lennard-Jones system is evaluated. Temperatures from $T^*=0.4$ up to $T^*=2.7$, with a grid step $\Delta T^*=0.1$ have been considered. In each isotherm several densities are simulated. The first corresponds to a density lower, but close to the solid density at which the solid–liquid equilibria occurs. The second chosen density is the solid density at melting. Higher densities (up to $\rho^{\mathrm{ref}}=1.25$) with a grid step $\Delta\rho^{\mathrm{ref}}=0.05$ are also studied. The overall density range is $0.90\leqslant\rho^{\mathrm{ref}}\leqslant 1.3$. In Fig. 1 the temperature–density states studied are indicated.

In order to have $g^{\mathrm{ref}}_{\mathrm{solid}}(\sigma)$ in the solid phase as a continuous function of the number density and temperature, the simulation data for $g^{\mathrm{ref}}_{\mathrm{solid}}(\sigma)$ are fitted to an empirical expression of the form proposed by Johnson *et al.*,[10] i.e.,

$$g^{\mathrm{ref}}_{\mathrm{solid}}(\sigma)=1+\sum_{i=1}^{5}\sum_{j=1}^{5}a_{ij}(\rho^{\mathrm{ref}})^i T^{*(1-j)}. \tag{8}$$

Hence, $g^{\mathrm{ref}}(\sigma)$ is given by Eq. (8) for the fluid and for the solid phase. In the fluid phase the parameters $a_{ij}$ used are those proposed by Johnson *et al.*,[10] while in the solid phase the parameters proposed in this work, which are given in Table I, are used. The $a_{ij}$ constants have been obtained using GAMS, a high-level modeling environment for mathematical programming problems.[36] The values of the pair radial distribution function at contact length obtained from the simulations are compared with the results of Eq. (8) in Fig. 2. In Fig. 2(a), $g^{\mathrm{ref}}_{\mathrm{solid}}(\sigma)$, as a function of reduced density, is shown for five isotherms. As can be seen, the radial distribution function at contact length is an increasing function of density, $(\partial g^{\mathrm{ref}}_{\mathrm{solid}}(\sigma)/\partial\rho^{\mathrm{ref}})_T>0$, in the range of densities covered by the simulations. This means that the contribution to the pressure due to chain formation in the solid phase is negative at all thermodynamic conditions considered. It can also be seen that Eq. (8) accurately reproduces the simulation data in our range of temperatures. The temperature dependence of $g^{\mathrm{ref}}_{\mathrm{solid}}(\sigma)$ for four isochores is presented in Fig. 2(b). The distribution function at contact length as a function of the temperature exhibits different behavior depending on the density considered. At the lowest densities studied ($\rho^{\mathrm{ref}}=1.0$ and 1.1) $g^{\mathrm{ref}}_{\mathrm{solid}}(\sigma)$ increases for increasing temperatures. Since the contribution to the internal configurational energy due to the chain formation in the solid phase is

TABLE I. Coefficients for the fit of $g^{\mathrm{ref}}_{\mathrm{solid}}(\sigma)$ as a function of temperature and density for the LJ solid monomer. The expression of the fit is that proposed by Johnson *et al.* (Ref. 10) [see Eq. (8) of the main text].

| $i$ | $j=1$ | $j=2$ | $j=3$ | $j=4$ | $j=5$ |
|---|---|---|---|---|---|
| 1 | −11.632 | 37.706 | −140.655 | 52.675 | 1.019 |
| 2 | 86.742 | −40.865 | 335.679 | −108.881 | −17.970 |
| 3 | −131.434 | −190.010 | −110.953 | −2.908 | 48.886 |
| 4 | 68.219 | 311.947 | −197.314 | 114.210 | −47.051 |
| 5 | −10.560 | −120.436 | 112.935 | −54.753 | 15.058 |

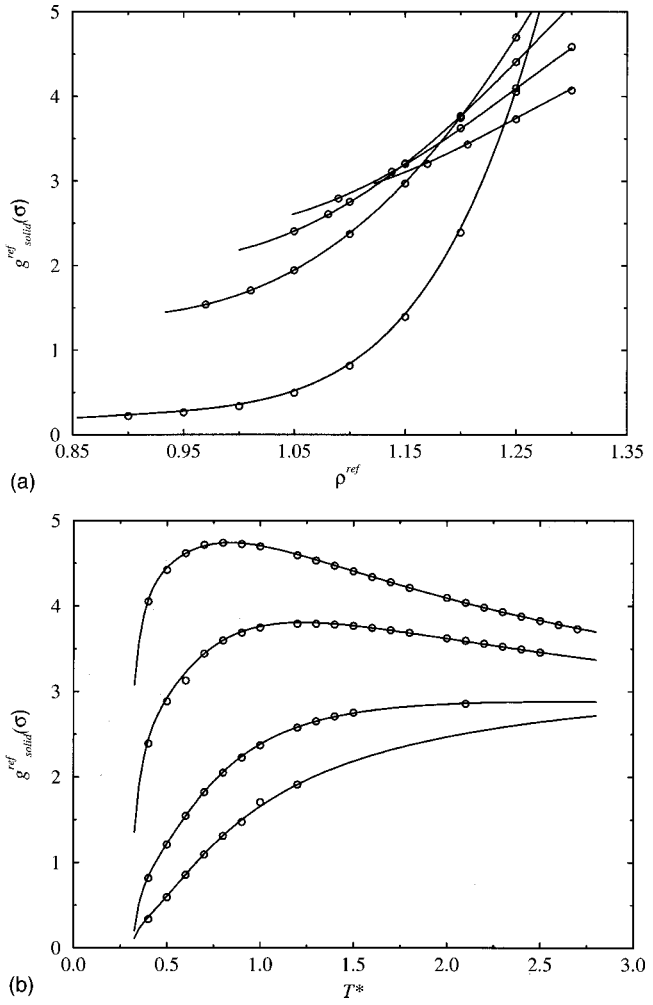


FIG. 2. $g^{\mathrm{ref}}_{\mathrm{solid}}(\sigma)$ of the LJ monomer solid as obtained from the *NVT* MC simulations of this work (symbols) and as given by the fit of Eq. (8) (solid curves). (a) Results for five isotherms. From bottom to top (on the left hand side) the results correspond to $T^*=0.4,1,1.5,2$, and 2.7, respectively. (b) Results for four isochores. From bottom to top the results correspond to $\rho^{\mathrm{ref}}=1,1.1,1.2,1.25$, respectively.

closely related with the first derivative of $g^{\mathrm{ref}}_{\mathrm{solid}}(\sigma)$ with respect to the temperature (at constant density), this contribution is positive at the lowest densities. At higher densities ($\rho^{\mathrm{ref}}=1.2$ to $\rho^{\mathrm{ref}}=1.25$) $g^{\mathrm{ref}}_{\mathrm{solid}}(\sigma)$ shows a more complicated behavior; at low temperatures it behaves as an increasing function of the temperature, a maximum is observed at intermediate temperatures, and at the highest temperatures it turns to a decreasing behavior. In summary, the contribution to the internal configurational energy due to the chain formation in the solid phase is negative at high temperatures and densities, and positive for all other thermodynamic conditions considered in our study.

### B. Computer simulations of the LJ dimer in the solid phase

In order to test the proposed theory we have performed $NpT$ Monte Carlo simulations of LJ dimer molecules in the solid phase. The reduced bond length of the dimer is $L^*=L/\sigma=1$, where $L$ is the bond length. In the Monte Carlo run three different types of moves were performed: particle translations, particle rotations, and volume changes. These three types of move leave the bond length unchanged. Notice that the LJ chains considered by Johnson *et al.*[10] in their molecular dynamics study used stiff springs to keep contiguous monomers bonded so that in their study the bond length is allowed to fluctuate around the equilibrium value $L=\sigma$. In our simulations a typical run consisted of 30 000 equilibration cycles and 30 000 averaging cycles, where a cycle consists of a trial move (translation or rotation) per particle plus an attempt to change the volume of the system. The magnitude of the displacement of the center of mass, angle of rotation and volume change was controlled to keep the acceptance ratio close to 0.4. Translation and rotation moves were accepted by following the standard Metropolis criterion.[35] The site–site LJ potential is truncated at $r_c=2.5\sigma$, and the long-range corrections to the internal energy are added as usual by assuming that the site–site pair correlation function is equal to one for distances larger than the cutoff value.[35] Note that in our $NpT$ simulations the long range correction to the energy was incorporated into the Markov chain (whenever the volume of the system changed), so that the output densities are good estimates of the corresponding densities of the system without truncation. A number of simulations with $r_c=3\sigma$ have also been carried out, finding no significant difference with the densities obtained using $r_c=2.5\sigma$.

In order to describe a disordered structure, a close-packed faced centered cubic (fcc) arrangement of atoms was generated and the molecular bonds were randomly distributed. That was done as follows. We generated a cubic hypercell by joining together eight face centered cubic unit cells of atoms. The number of atoms per hypercell is 32 (1 in the vertex, 15 in the faces, 3 in the edges, and 13 inside). We connected the 32 atoms randomly, forming 16 dimers. The simulation box was obtained by joining together 27 such hypercells. Therefore the total number of molecules in the $NpT$ MC simulations of the disordered structure was $N=432$ (27 hypercells with 16 dimers each). Disordered solid configurations similar to those considered here, are also found in two-dimensional hard dimer discs[28,29,37] and in hard sphere chain[19] systems. Note also that there is no true close packing for a soft potential such as the LJ but the reduced number density of hard spheres at close packing, i.e., $\sqrt{2}$, provides a good starting point. This disordered structure was expanded to lower densities by performing $NpT$ simulations at successively decreasing pressures. In order to assess the influence of generating different starting random solid configurations a second random structure was generated, then carrying out a number of $NpT$ simulations in an identical way. It is important to note that, since the distribution of bonds in the solid phase is assumed isotropic, the scaling in these $NpT$ simulations was done isotropically. In what follows the reduced configurational internal energy will be given as $U^*=U/(N\epsilon)$ (note that $N$ corresponds to the number of molecules, and not the number of segments). The simulation results in this work were obtained for two isotherms $T^*=1$ and $T^*=2$. In Table II the simulation results for the disordered solid phase at $T^*=1$ are shown. The results presented are the average of the runs for two independent disordered configurations. For a number of pressures the typical difference between the properties of the two independent configurations are indicated in parentheses. As can be seen the differences in thermodynamic properties between

TABLE II. Thermodynamic properties of a LJ dimer in a disordered solid phase as obtained from the $NpT$ MC simulations of this work. The results correspond to $T^*=1$. The results presented are the arithmetic average of the results for two independent disordered configurations. The reduced pressure is defined as $p^*=p/(\epsilon/\sigma^3)$. The reduced number density of dimers is defined as $\rho=N\sigma^3/V$. $N$ stands for the number of molecules. The blank line separates the results of the isotropic fluid from those of the solid phase. For a few states we have presented in parentheses the difference between the results of the two independent disordered configurations.

| $p^*$ | $\rho$ | $U/(N\epsilon)$ |
|---|---|---|
| 0.6 | 0.4255 | −10.99 |
| 0.8 | 0.4309 | −11.12 |
| 1.0 | 0.4353 | −11.22 |
| 1.2 | 0.4396 | −11.31 |
| 1.4 | 0.4432 | −11.39 |
| 1.6 | 0.4973 | −13.15 |
| 1.8 | 0.5002 | −13.19 |
| 2 | 0.5047 | −13.29 |
| 3 | 0.5197(4) | −13.57(4) |
| 4 | 0.5314 | −13.74 |
| 6 | 0.5490 | −13.89 |
| 8 | 0.5626 | −13.92 |
| 10 | 0.5738(5) | −13.88(3) |
| 12 | 0.5835 | −13.78 |
| 14 | 0.5921 | −13.65 |
| 16 | 0.6001 | −13.49 |
| 18 | 0.6074 | −13.30 |
| 20 | 0.6142(3) | −13.10(3) |
| 25 | 0.6297 | −12.53 |
| 30 | 0.6431 | −11.90 |
| 35 | 0.6549 | −11.23 |
| 40 | 0.6656 | −10.54 |
| 45 | 0.6751(1) | −9.83(2) |
| 50 | 0.6838 | −9.12 |
| 55 | 0.6917 | −8.39 |

TABLE III. Thermodynamic properties of a LJ dimer in a disordered solid phase as obtained from the $NpT$ MC simulations of this work. The results correspond to $T^*=2$. The rest of the notation is as in Table II. The blank line separates the results of the isotropic fluid from those of the solid phase.

| $p^*$ | $\rho$ | $U/(N\epsilon)$ |
|---|---|---|
| 0.6 | 0.2912 | −6.72 |
| 0.8 | 0.3096 | −7.17 |
| 1.0 | 0.3226 | −7.47 |
| 1.2 | 0.3335 | −7.73 |
| 1.4 | 0.3427 | −7.95 |
| 1.6 | 0.3511 | −8.14 |
| 1.8 | 0.3584 | −8.30 |
| 2 | 0.3652 | −8.45 |
| 4 | 0.4113 | −9.37 |
| 6 | 0.4401 | −9.81 |
| 8 | 0.4619 | −10.03 |
| 10 | 0.4800 | −10.15 |
| 12 | 0.5373 | −11.68 |
| 14 | 0.5526 | −11.77 |
| 16 | 0.5658 | −11.78 |
| 18 | 0.5763 | −11.72 |
| 20 | 0.5854 | −11.60 |
| 25 | 0.6049 | −11.20 |
| 30 | 0.6209 | −10.69 |
| 35 | 0.6346 | −10.09 |
| 40 | 0.6470 | −9.47 |
| 45 | 0.6579 | −8.80 |
| 50 | 0.6679 | −8.10 |
| 55 | 0.6770 | −7.39 |
| 60 | 0.6853 | −6.67 |

TABLE IV. Thermodynamic properties of a LJ dimer in an ordered solid phase as obtained from the $NpT$ MC simulations of this work. The results correspond to $T^*=1$. The solid structure used in the simulations is that denoted as CP1 in Ref. 38. The rest of the notation is as in Table II. Results of this table were obtained with $N=256$. In a few cases (labeled with an asterisk) we considered $N=500$ to analyze the system size dependence.

| $p^*$ | $\rho$ | $U/(N\epsilon)$ |
|---|---|---|
| 0.6 | 0.4256 | −10.99 |
| 0.8 | 0.4307 | −11.12 |
| 1.0 | 0.4349 | −11.21 |
| 1.2 | 0.4827 | −13.09 |
| 1.4 | 0.4904 | −13.34 |
| 1.6 | 0.4951 | −13.48 |
| 1.8 | 0.4991 | −13.58 |
| 2 | 0.5010 | −13.59 |
| 2* | 0.5029 | −13.67 |
| 3 | 0.5153 | −13.91 |
| 4 | 0.5263 | −14.08 |
| 6 | 0.5434 | −14.25 |
| 6* | 0.5437 | −14.26 |
| 8 | 0.5569 | −14.30 |
| 10 | 0.5683 | −14.27 |
| 10* | 0.5684 | −14.27 |
| 12 | 0.5781 | −14.18 |
| 14 | 0.5869 | −14.06 |
| 16 | 0.5947 | −13.91 |
| 18 | 0.6020 | −13.73 |
| 20 | 0.6090 | −13.53 |
| 20* | 0.6090 | −13.53 |
| 25 | 0.6243 | −12.96 |
| 30 | 0.6382 | −12.31 |
| 30* | 0.6382 | −12.31 |
| 35 | 0.6505 | −11.61 |
| 40 | 0.6617 | −10.88 |
| 40* | 0.6618 | −10.88 |
| 45 | 0.6718 | −10.14 |
| 50 | 0.6812 | −9.36 |
| 50* | 0.6812 | −9.36 |
| 55 | 0.6898 | −8.57 |
| 60 | 0.6978 | −7.78 |
| 60* | 0.6978 | −7.78 |

the two independent configurations are very small. At pressures below $p^*=1.6$ the solid phase becomes mechanically unstable and melts into an isotropic fluid. The melting is detected by a sudden drop of the translational order parameter,[35] by an increase in the molecular diffusion and by a strong increase in the volume of the simulation box. We use the location of the atoms (and not of the center-of-masses) when evaluating the translational order parameter. In Table III the simulations results for $T^*=2$ are presented. Since the differences between the two disordered configurations at $T^*=1$ are small we have performed simulations at $T^*=2$ for just one of them. At this temperature the solid phase becomes mechanically unstable and melts into an isotropic fluid at pressures below $p^*=12$.

Although the stable solid structure of the dimer system must be a disordered one, we have also considered an ordered structure. It is interesting to study the differences in thermodynamic properties between an ordered and a disordered dimer solid. In particular we have considered the structure labeled as CP1 in a previous study of hard dumbbells in the solid phase.[38] In this case $N=256$ molecules arranged in four layers with 64 molecules per layer were used. For a few states we performed simulations for a somewhat larger system $N=500$ in the CP1 structure (5 layers of 100 molecules each), to analyze the size dependence of the simulation results. As before, the length of the runs was of 30 000 equilibration cycles, followed by 30 000 averaging cycles. Since in this case the system is no longer cubic, the Rahman–Parrinello[39] version of the $NpT$ MC is used in order to allow for nonisotropic changes in the simulation box shape.[40] In Table IV the simulation results for this system at $T^*=1$ are presented. As can be seen the size dependence of the simulation results is quite small. By comparing the results of Table IV to those of Table II it can be seen that the thermodynamic properties of the ordered and disordered solid are similar. At a given pressure, the densities of the disordered solid are about 1% higher than those of the ordered solid, and the internal energies of the disordered solid are also slightly higher than those of the ordered solid. These results are in agreement with those of Wojciechowski *et al.*,[28] who found little difference between the EOS of ordered and disordered solids in hard disc dimers (i.e., in a two-dimensional system). It is important to note however, that although the EOS and internal energy of the ordered and disordered structures are quite similar this is not the case for the entropy, which is much higher for the disordered structure.[28,29] Hence, the Helmholtz free energy of the disordered solid is significantly lower than that of the ordered solid, so that the equilibrium structure of the LJ dimer in the solid phase cor-

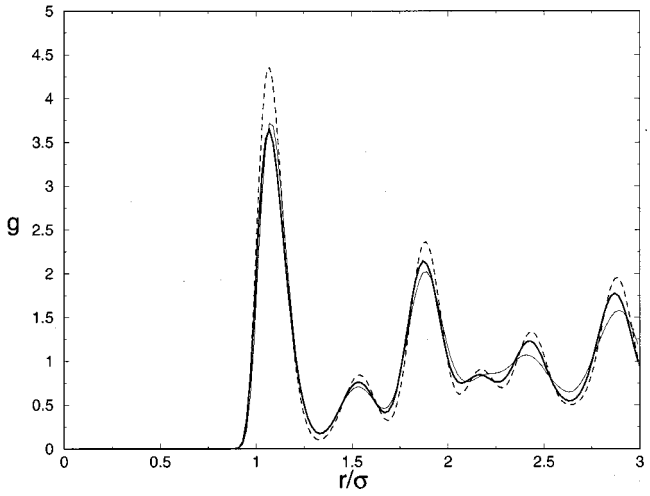


FIG. 3. Site–site correlation functions in the solid phase at $T^*=1$ as obtained from Monte Carlo simulations. The results for the dimer $m=2$ at $\rho=0.545$ in the disordered solid (thick solid curve) and in the ordered solid (thin solid curve) are shown. The results for the LJ monomer in the solid phase at the same monomer density $\rho^{\mathrm{ref}}=1.09$ are also presented (dashed curve).

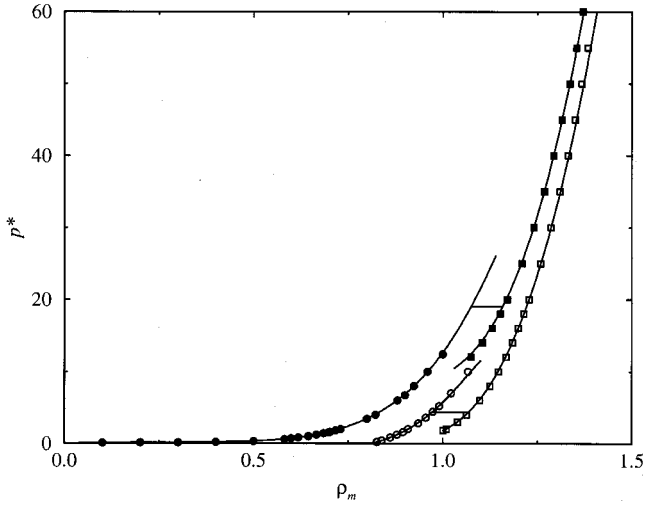


FIG. 4. Equation of state for the LJ dimer as given by the theory (curves) and by simulation results from this work (symbols). Results are presented for the fluid and solid phases at the reduced temperatures $T^*=1$ and $T^*=2$. The open symbols correspond to the simulation data at a temperature of $T^*=1$, and the closed symbols to $T^*=2$. The circles indicate fluid states and the squares solid states. The tie-lines represent the fluid–solid coexistence as determined from TPT1, which occur at $p^*=4.35$ and $p^*=19.02$ for $T^*=1$ and $T^*=2$, respectively. For $T^*=2$ we have also included simulation results from Ref. 10 for the fluid phase.

responds to the disordered solid, and not to the ordered solid.

The structural properties of the disordered and ordered dimer solids were also analyzed. In Fig. 3 the site–site correlation functions as obtained from MC simulations for $T^*=1$ and $\rho=0.545$ are presented for the disordered solid (thick solid curve), and for the ordered solid (thin solid curve). Differences between the two types of solid are clearly visible at large distances, and in the first peak. The atom–atom correlation function of the LJ monomer solid at the same temperature and monomer density ($\rho^{\mathrm{ref}}=1.09$) is also shown (dashed curve). The comparison between the site–site correlation function of the dimer and the atom–atom correlation function of the monomer illustrates the effect of bonding on the structure of the system.

We have also performed a number of simulations for the dimer LJ system at very low temperatures and zero pressure, since an estimate of the solid densities along the sublimation curve can be obtained by performing $NpT$ simulations at zero pressure. These results are presented in Table V for the disordered solid and for the CP1 structure.

TABLE V. Properties of the LJ dimer in the solid phase along the sublimation line, as obtained from $NpT$ simulations at zero pressure. Results for an ordered and disordered structure are presented.

| $T^*$ | Solid | $\rho$ | $U/(N\epsilon)$ |
|---|---|---|---|
| 0.40 | Disordered | 0.5380 | −15.17 |
| 0.45 | Disordered | 0.5340 | −15.00 |
| 0.50 | Disordered | 0.5296 | −14.83 |
| 0.55 | Disordered | 0.5250 | −14.65 |
| 0.60 | Disordered | 0.5199 | −14.45 |
| 0.65 | Disordered | 0.5144 | −14.24 |
| 0.40 | CP1 | 0.5343 | −15.50 |
| 0.50 | CP1 | 0.5260 | −15.16 |
| 0.55 | CP1 | 0.5216 | −14.98 |
| 0.60 | CP1 | 0.5169 | −14.79 |
| 0.65 | CP1 | 0.5118 | −14.59 |

In the following section our simulation data of the dimer LJ solid are compared with the theoretical calculations, in all cases the simulation results correspond to those of the disordered solid, as this is the true equilibrium structure of the model.

## IV. THE PHASE DIAGRAM OF THE LENNARD-JONES DIMER

An unbiased assessment of the equation of state proposed can be obtained by comparison with the presented simulation data for the dimer LJ system. It is important to note that the equation of state described in Sec. II corresponds to that of a solid with a fcc structure of monomers, but with random orientation of the bond vectors (a disordered solid). Hence we have used the data in Tables II, and III for comparison, but not those of Table IV. The EOS for two isotherms ($T^*=1$ and $T^*=2$) is examined in Fig. 4. At each temperature the fluid branch can be seen at lower densities and the solid branch at higher densities, together with a first-order fluid–solid transition. The simulation results present hysteresis, so that it is possible to simulate the solid for pressures lower than that of melting, and the fluid for pressures higher than that of freezing. In the case of the theoretical calculations, the conditions for equilibria (equality of pressure and chemical potential) were solved for each temperature, and the calculated coexistence pressures for each temperature can be seen in Fig. 4. The metastable branches obtained with the equation of state are also presented for comparison with the simulated data. A further test of the theory is provided by an examination of the internal energy. In Fig. 5 the simulation data of the internal energy of the dimer are compared to the theoretical predictions for temperatures $T^*=1$ and $T^*=2$. The agreement between the

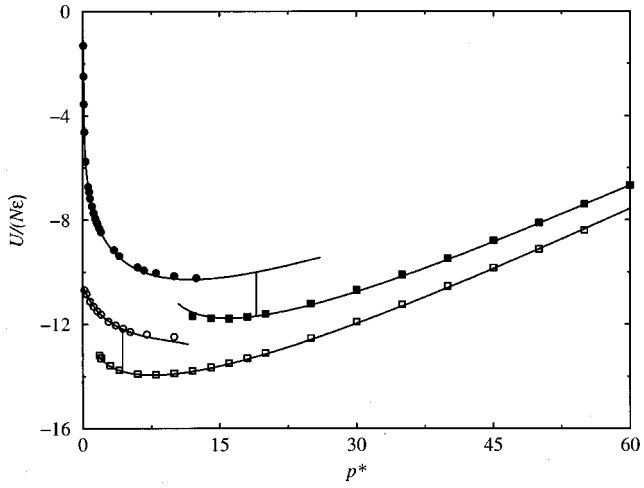


FIG. 5. Configurational internal energy $U/(N\epsilon)$ for the LJ dimer as given by the theory (curves) and by simulation results from this work (symbols). Results are presented for the fluid and solid phases at the reduced temperatures $T^*=1$ and $T^*=2$. The rest of the notation is as in Fig. 4. For $T^*=2$ we have also included simulation results from Ref. 10 for the fluid phase.

simulation data and the calculations is found to be very good over the wide range of densities considered, both for the equation of state data, and for the internal energy data.

In Fig. 6(a) the global phase diagram for the LJ dimer as obtained from Wertheim's TPT1 for the fluid and solid phase is presented. The Gibbs ensemble simulation data for the vapor–liquid equilibria of the LJ dimer as reported by Dubey *et al.*[41] have been included, together with our simulation results for the zero-pressure densities of the LJ dimer solid at low temperatures. Since the vapor–pressure (in reduced units) is very small along the vapor–solid coexistence curve, these simulations provide a good estimate of the solid densities along the sublimation curve. As can be seen, the theory describes very accurately the available simulation results of the phase diagram of the LJ dimer. The triple point temperature for the LJ dimer as estimated from the theory presented in this work is $T_t^*=0.653$. In the case of the monomer LJ system, the triple point temperature predicted by the theory ($T_t^*=0.687$) is in excellent agreement with the estimate of Agrawal and Kofke[42] ($T_t^*=0.687$). As can be seen, the triple point temperature of the LJ dimer is 5% lower than that of the LJ monomer. Differences in the triple point densities are somewhat larger, as can be seen in Fig. 6(b). Following the encouraging results obtained for the dimer system we continue, in the next section, to study the phase behavior of longer chain molecules.

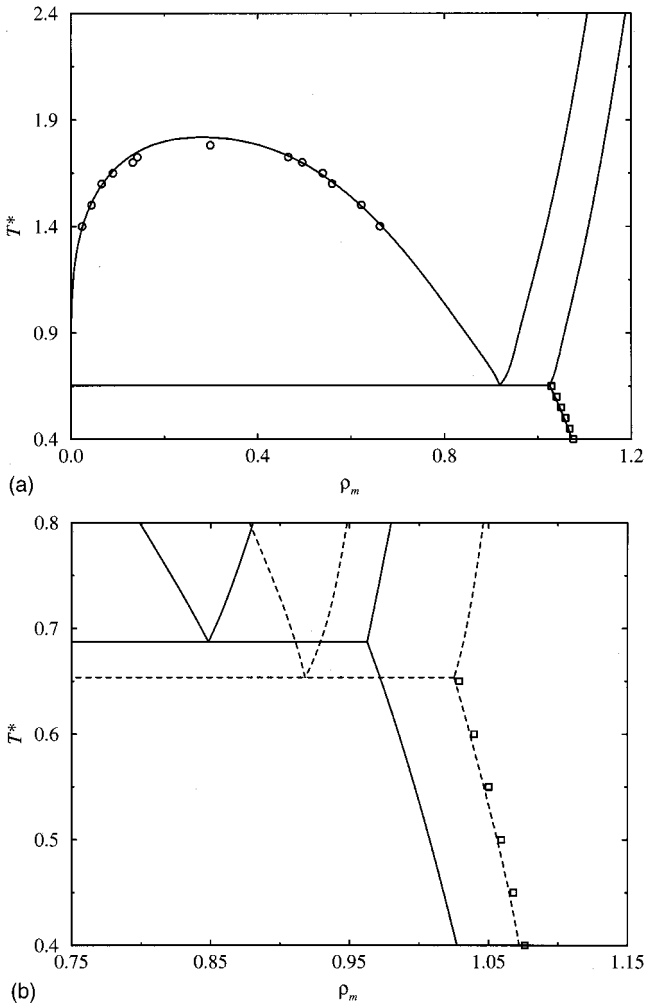


FIG. 6. (a) Global phase diagram of the LJ dimer in the $T^*$ vs $\rho_m$ representation. Solid line, theoretical results from this work using Wertheim's TPT1 for the fluid and solid phases; circles, simulation results for the vapor–liquid equilibria from Dubey *et al.* (Ref. 41); squares, simulation results for the sublimation line from this work. (b) Triple point region of the LJ dimer (dashed line) and monomer (solid line) as obtained from the theory of this work.

## V. GLOBAL PHASE DIAGRAM FOR LJ CHAINS

Using the theory presented in Sec. II, we have also studied the phase behavior of fully-flexible Lennard-Jones chains of lengths $m=4$ and $m=8$. In Fig. 7(a) the temperature–density ($T^*\rho_m$) projection of the phase diagram is shown, where, as in the previous section, the reduced density corresponds to the reduced monomer density. The phase envelope corresponding to the monomer $m=1$ and dimer $m=2$ Lennard-Jones systems are included for comparison. As expected, an increase of the chain length results in a more dramatic variation of the vapor–liquid coexistence than of the solid–liquid and solid–gas phase boundaries. Since the theoretical predictions corresponding to the fluid phases have been discussed in detail elsewhere (see Refs. 13–15), in this work we concentrate on the study of the solid–fluid equilibria. For each chain length, the liquid–solid transition densities are found to increase with temperature. The increase is more pronounced in the monomer system than for longer chains. The temperature at which solid, liquid, and gas are found in coexistence (the triple point temperature) is seen to decrease with increasing chain length [see Fig. 7(b) and Table VI for more details]. Below the triple point temperature, solid–gas coexistence is observed. The binodal curves corresponding to the solid phase associated to the solid–gas phase transition shift toward higher densities for increasing chain length. As in the case of the solid–liquid coexistence curves, the largest change in the solid–gas phase boundaries is observed between the monomer and the dimer.

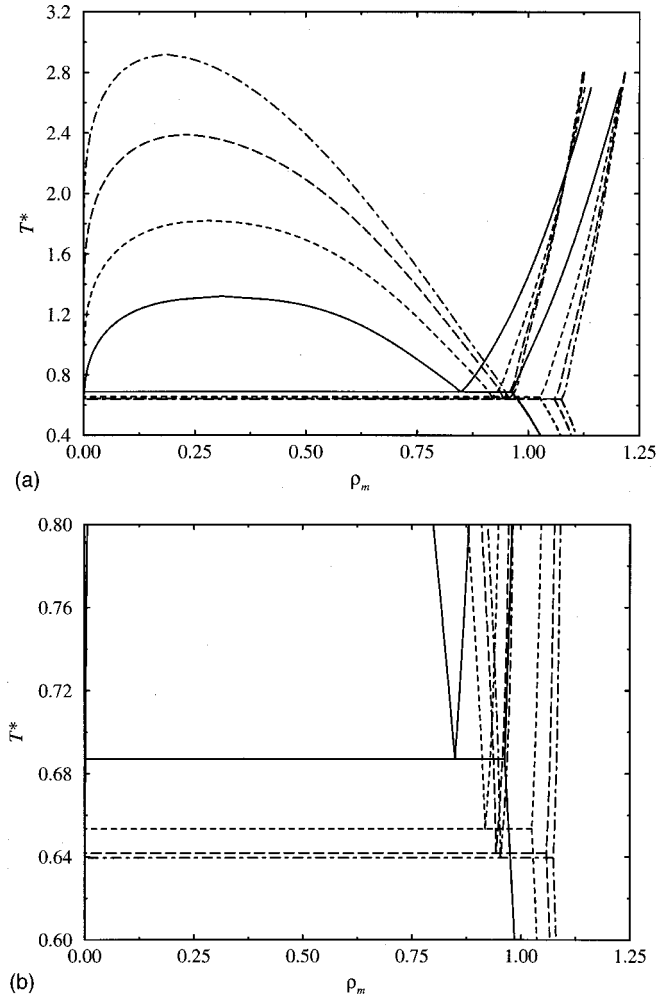


FIG. 7. $T^*\rho_m$ global phase diagram for LJ chains of chain lengths $m=1,2,4$ and 8, as obtained from the theory presented in this work. The solid curves correspond to $m=1$, the short dashed curves to $m=2$, the long dashed curves to $m=4$, and the dashed–dotted curves to $m=8$. (a) Global phase diagram. (b) The region close to the triple point.

The results of Fig. 7 strongly indicate the existence of asymptotic limits in the freezing properties of LJ chains for large values of $m$. In fact, they suggest that the triple point temperature and the fluid–solid coexistence densities (when expressed in monomer units $\rho_m$) become independent of the chain length for large values of $m$. These observations are a direct result of the functional form of the Helmholtz free energy in Wertheim's TPT1 approach. In Wertheim's formalism, the compressibility factor $Z$ and chemical potential $\mu/(kT)$ can be written as[26]

TABLE VI. Triple point properties of fully flexible LJ chains as obtained from Wertheim's TPT1 for the fluid and solid phases. The coexistence densities of the fluid and solid phases are denoted as $\rho_{mf}$ and $\rho_{ms}$, respectively.

| $m$ | $T_t^*$ | $p^*$ | $\rho_{mf}$ | $\rho_{ms}$ |
|---|---|---|---|---|
| 1 | 0.687 | $1.15\times10^{-3}$ | 0.848 | 0.963 |
| 2 | 0.653 | $8.13\times10^{-7}$ | 0.918 | 1.025 |
| 4 | 0.642 | $9.97\times10^{-13}$ | 0.943 | 1.059 |
| 8 | 0.639 | $4.28\times10^{-24}$ | 0.953 | 1.074 |

$$X(\rho_m,T,m)=X_1(\rho_m,T)+mX_2(\rho_m,T), \tag{9}$$

where $X$ stands for any of the thermodynamic properties [$Z$ or $\mu/(kT)$]. Since this is true for the fluid and the solid phase, the equilibrium condition for, say, the chemical potential between the fluid and solid phase (superscript $f$ and $s$, respectively) may be expressed as

$$\frac{\mu_1^f(\rho_{mf},T)}{m}+\mu_2^f(\rho_{mf},T)=\frac{\mu_1^s(\rho_{ms},T)}{m}+\mu_2^s(\rho_{ms},T), \tag{10}$$

where $\rho_{mf}$ and $\rho_{ms}$ stand for the monomer number density in the fluid and in the solid phase at coexistence. For sufficiently large values of $m$, Eq. (10) reads as

$$\mu_2^f(\rho_{mf},T)=\mu_2^s(\rho_{ms},T), \tag{11}$$

which is independent of $m$. Similarly, starting from Eq. (9) for the compressibility factor, and imposing the condition of equal pressure for the fluid and solid phases, one can show that the reduced pressure $p^*$ at coexistence becomes independent of $m$ in the infinite-chain limit (see Ref. 26 for more details).

From the results of Fig. 7 the triple point of LJ chains in the limit $m\to\infty$ can be estimated close to $T_t^*=0.634$ (performing, for instance, a Shultz–Flory extrapolation[43,44]). The existence of an asymptotic limit in the triple point temperature for long polymer chains is experimentally well known. In fact the triple point temperature of $n$-alkanes reaches the asymptotic value $T_t=414$ K (Refs. 25 and 45) for large molecular weights. When modeling $n$-alkanes with tangent LJ chains the value of the parameter $\epsilon/k$ is close to 300 K.[46] This means that the reduced temperature of $n$-alkanes at the experimental triple point is roughly $T_t^*=1.38$. As it can be seen the reduced triple point temperature of LJ chains is quite different of the reduced triple point temperature of $n$-alkanes. It seems that a fully-flexible LJ chain is not particularly adequate to describe $n$-alkanes in the solid phase. We shall come back to this point later in this work. The fluid densities at the triple point in $n$-alkane systems also reach asymptotic values for large molecular weights (when expressed as masses per unit of volume). It is gratifying to see that the theory is able to explain the origin of these limiting behaviors. However, the liquid range of the fully flexible LJ chains seems to be extremely large. In fact since the critical temperature of infinitely long LJ chains[47,32] (i.e., the $\Theta$ temperature) is close to $T^*=4.6$, so that the ratio $T_t/T_c$ for LJ chains is of the order of 0.14. One of the liquids with a largest liquid regime is propane, for which $T_t/T_c=0.23$, and in a spherical fluid such as argon, this ratio is about 0.55; this provides an idea of the extraordinary liquid regime presented by these LJ chains. It is not easy to describe trends in $T_t/T_c$ for molecular fluids. Considerable effort has been devoted in the last decade to explain this ratio in a number of molecular fluids.[48,49,18] Can we provide a qualitative explanation of the origin of the value 0.14 for $T_t/T_c$ in fully-flexible LJ chains? The critical temperature of LJ chains increases from $T^*=1.31$ for the monomer up to about 3.5 times this value for very long chains. This is a huge variation. However, the triple point temperature of very long chains is just 0.93 times

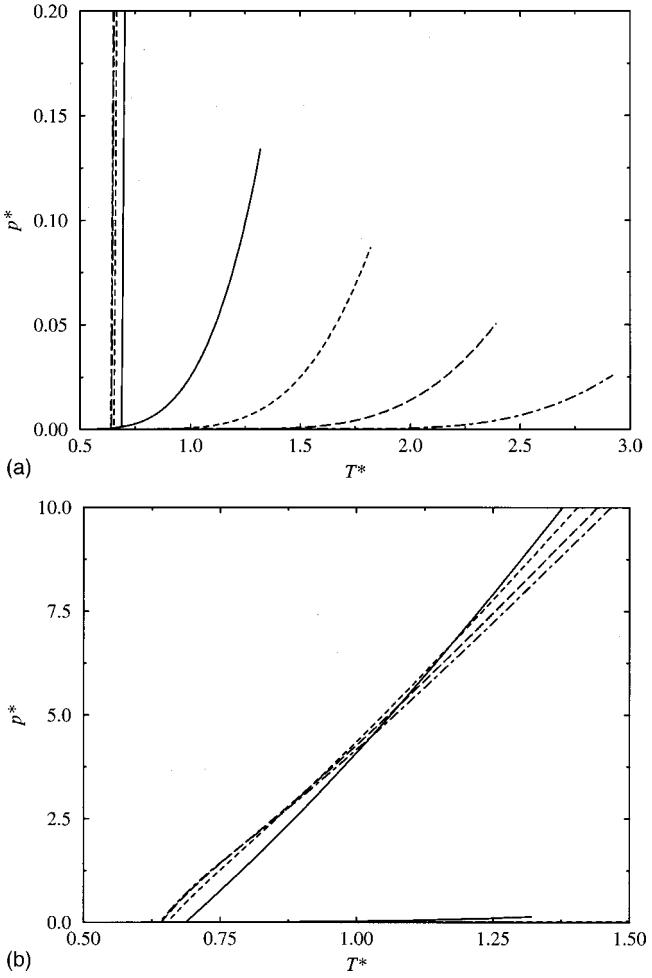


FIG. 8. $p^*T^*$ representation of the global phase diagram for LJ chains with $m=1,2,4$, and 8 as obtained from the theory presented in this work. The solid curves correspond to $m=1$, the short dashed curves to $m=2$, the long dashed curves to $m=4$, and the dashed–dotted curves to $m=8$. (a) Low pressure region. (b) High pressure region.

that of the LJ monomer. One can understand easily the enormous increases of the critical temperature of LJ chains with respect to the monomer. How to understand the almost constant value for the triple point temperature? As can be seen in Fig. 7, at low temperatures the increase of the orthobaric density from $m=1$ to $m=2$ is almost identical to the increase in the density at freezing from $m=1$ to $m=2$, so that the triple point temperature remains practically unaffected. Of course this is not exact, but it provides a simple view as to why the triple point temperature is approximately constant.

It is useful to examine also the $p^*T^*$ projection of the phase diagram as obtained with the theoretical approach (see Fig. 8). In Fig. 8(a) the vapor–pressure curve, solid–liquid transition line, and solid–gas transition line corresponding to freely-jointed Lennard-Jones chains of up to eight monomers ($m=8$) are presented. The coexistence lines of the Lennard-Jones monomer system are included for comparison. It is more interesting to analyze the high-pressure region of the $p^*T^*$ projection of the phase diagram [Fig. 8(b)]. The liquid–vapor and solid–gas coexistence curves cannot be seen in this plot since these boundaries occur at very low pressures compared to the range at which solid–liquid transition continues. As can be seen, at low temperatures the fluid–solid transition pressures increase with increasing $m$, however, at high temperatures this trend is inverted, and the solid–liquid transition pressures decrease for increasing chain lengths. The slope in the $p^*T^*$ is related to the melting enthalpy and to the volume change through the Clapeyron equation.[50]

## VI. CONCLUSIONS

In this work Wertheim's TPT1 theory has been extended to study the solid phase of LJ chains. The theory requires a knowledge of the free energy and of the contact value of the radial distribution function of the reference LJ monomer. Johnson *et al.*[9,10] have given expressions for both of these properties in the fluid phase, and van der Hoef[34] has recently proposed an expression for the free energy of the solid phase. In order to determine $g^{\mathrm{ref}}(\sigma)$ in the solid phase we have performed computer simulations and fitted the numerical results to an empirical expression of the same form as that proposed by Johnson *et al.*[10] The theory has been tested by comparing simulation and theoretical results for the LJ dimer. For this purpose computer simulations were performed for the disordered solid structure of the LJ dimer. It has been shown that the theory describes very accurately the EOS and internal energy of the LJ dimer solid. Furthermore, the densities of the solid along the sublimation curve are also found to be in excellent agreement with simulation data. Our estimate of the triple point temperature for the LJ dimer is $T_t^*=0.653$. Using Wertheim's TPT1 for the fluid and for the solid phase we have calculated the vapor–liquid, liquid–solid, and solid–vapor coexistence lines as well as the global phase diagram of LJ chains.

Studying longer chain molecules, it has been shown that the calculated triple point temperature of LJ chains tends to an asymptotic finite value of $T_t^*=0.634$, which means that the chains present an enormous liquid range (i.e., $T_t/T_c=0.14$). The calculated coexistence densities (when expressed in monomers per unit of volume $\rho_m$) also tend to asymptotic values for large values of $m$. Although the model used in this work is a crude one, it is able to capture some of the features presented in the phase diagram of real flexible molecules. In polyethylene the triple point temperature reaches a finite value and the fluid–solid coexistence densities become very similar for large chain lengths (when the densities are expressed in units of mass per volume).

It should be noted, however, that fully flexible models may not be particularly realistic when describing solid phases of real substances. The extreme flexibility of the LJ chain allows the existence of a singular solid with ordering of atoms but disorder of bonds. It must be mentioned that such a solid cannot be constructed using real polymers; overlap between contiguous monomers, whose distance is less than the sum of their van der Waals radii, and the existence of bond angles and torsional potentials make such a high-density disordered solid an impossibility. When these geometrical constraints are included in the model, the only way of obtaining a highly-packed solid is to generate an ordered

solid, in which the bonds are also ordered. Certainly, real chains are not formed by fully flexible tangent LJ segments; this is reflected in the fact that the $T_t/T_c$ ratio for polyethylene[51] is close to 0.40 (with some recent estimates of $T_c$ of polyethylene[52] this ratio will be somewhat smaller, namely, 0.34) in contrast to the value $T_t/T_c=0.14$ obtained in this work using fully flexible LJ chains. Obviously, chemical and geometrical details of the molecule matter when dealing with the description of solid phases. The fully flexible LJ model does not seem to be the most appropriate model to describe the solid structure of *n*-alkanes. This was not our goal here, but rather to determine the phase diagram of LJ chains in a full theoretical manner, and to show that a very simple model can be useful in explaining some of the trends (not the actual values) in a number of properties of the phase diagram of real polymers.

Concerning the issue of whether the theory presented here could be useful, in an engineering sense, to describe the global phase behavior (vapor–liquid, vapor–solid, liquid–solid equilibrium) of real chains, we believe that the answer is, in principle, no. One cannot reproduce the value $T_t/T_c=0.4$ of polyethylene[51] with a model that yields $T_t/T_c=0.14$. The freely jointed LJ chain is not a good model for an *n*-alkane after all. A look at the important differences in the freezing properties of freely jointed hard sphere chains and hard models of *n*-alkanes with a realistic description of the molecular shape already suggests this.[19,20] This paper provides further evidence. Although we can describe *n*-alkanes in the fluid phase using a freely jointed LJ chain model, after fitting all the parameters to experimental properties, the model will never be able to describe correctly the global phase diagram of an *n*-alkane (including solid phases). If a model is required to describe the complete phase diagram of *n*-alkanes, models such as the Ryckaert and Bellemans,[53] and their modern variations,[54–56] which include the geometrical details of the molecule, might be more promising. Maybe a less ambitious approach is possible if one allows a different set of potential parameters for the fluid and the solid phase, or if a set of potential parameters is used solely to describe the solid phase. This does not seem to be justified from a molecular point of view (molecular parameters of the potential should be the same in the fluid and solid phase) but could be of interest for practical applications.

## ACKNOWLEDGMENTS

Financial support is due to Project No. BFM-2001-1420-C02-01 and BFM-2001-1420-C02-02 of the Spanish DGICYT (Dirección General de Investigación Científica y Técnica). F.J.B. would like to acknowledge the Universidad de Huelva and Junta de Andalucía for additional financial support. A.G. would like to thank the Engineering and Physical Sciences Research Council for the award of an Advanced Research Fellowship.

[1] M. S. Wertheim, J. Stat. Phys. **35**, 19 (1984).
[2] M. S. Wertheim, J. Stat. Phys. **35**, 35 (1984).
[3] M. S. Wertheim, J. Stat. Phys. **42**, 459 (1986).
[4] M. S. Wertheim, J. Stat. Phys. **42**, 477 (1986).
[5] M. S. Wertheim, J. Chem. Phys. **85**, 2929 (1986).
[6] M. S. Wertheim, J. Chem. Phys. **87**, 7323 (1987).
[7] W. G. Chapman, G. Jackson, and K. E. Gubbins, Mol. Phys. **65**, 1057 (1988).
[8] W. G. Chapman, J. Chem. Phys. **93**, 4299 (1990).
[9] J. K. Johnson, J. A. Zollweg, and K. E. Gubbins, Mol. Phys. **78**, 591 (1993).
[10] J. K. Johnson, E. A. Müller, and K. E. Gubbins, J. Phys. Chem. **98**, 6413 (1994).
[11] A. Gil-Villegas, A. Galindo, P. J. Whitehead, S. J. Mills, G. Jackson, and A. N. Burgess, J. Chem. Phys. **106**, 4168 (1997).
[12] L. A. Davies, A. Gil-Villegas, and G. Jackson, J. Chem. Phys. **111**, 8659 (1999).
[13] F. A. Escobedo and J. J. de Pablo, Mol. Phys. **87**, 347 (1996).
[14] F. J. Blas and L. F. Vega, Mol. Phys. **92**, 1 (1997).
[15] F. J. Blas and L. F. Vega, J. Chem. Phys. **115**, 4355 (2001).
[16] L. G. MacDowell, M. Müller, C. Vega, and K. Binder, J. Chem. Phys. **113**, 419 (2000).
[17] C. T. Lin and G. Stell, J. Chem. Phys. **114**, 6969 (2001).
[18] P. A. Monson and D. A. Kofke, Adv. Chem. Phys. **115**, 113 (2000).
[19] A. P. Malanoski and P. A. Monson, J. Chem. Phys. **107**, 6899 (1997).
[20] A. P. Malanoski and P. A. Monson, J. Chem. Phys. **110**, 664 (1999).
[21] J. M. Polson and D. Frenkel, J. Chem. Phys. **109**, 318 (1998).
[22] J. M. Polson and D. Frenkel, J. Chem. Phys. **111**, 1501 (1999).
[23] R. P. Sear and G. Jackson, J. Chem. Phys. **102**, 939 (1995).
[24] A. P. Malanoski, C. Vega, and P. A. Monson, Mol. Phys. **98**, 363 (2000).
[25] R. C. Reid, J. M. Prausnitz, and B. E. Poling, *The Properties of Gases and Liquids*, 4th ed. (McGraw–Hill, New York, 1987).
[26] C. Vega and L. G. MacDowell, J. Chem. Phys. **114**, 10411 (2001).
[27] C. McBride and C. Vega, J. Chem. Phys. **116,** 1757 (2002).
[28] K. W. Wojciechowski, A. C. Branka, and D. Frenkel, Physica A **196**, 519 (1993).
[29] K. W. Wojciechowski, D. Frenkel, and A. C. Branka, Phys. Rev. Lett. **66**, 3168 (1991).
[30] Y. Zhou and G. Stell, J. Chem. Phys. **96**, 1507 (1992).
[31] W. R. Smith, I. Nezbeda, M. Strnad, B. Triska, S. Labik, and A. Malijevsky, J. Chem. Phys. **109**, 1052 (1998).
[32] C. Vega and L. G. MacDowell, Mol. Phys. **98**, 1295 (2000).
[33] D. A. McQuarrie, *Statistical Mechanics* (Harper and Row, New York, 1976).
[34] M. A. van der Hoef, J. Chem. Phys. **113**, 8142 (2000).
[35] M. P. Allen and D. J. Tildesley, *Computer Simulation of Liquids*, 2nd ed. (Clarendon, Oxford, 1987).
[36] A. Brooke, D. Kendrick, A. Meeraus, and R. Raman, GAMS, A User's Guide, GAMS Development Corporation.
[37] R. Bowles and R. J. Speedy, Mol. Phys. **87**, 1349 (1996).
[38] C. Vega, E. P. A. Paras, and P. A. Monson, J. Chem. Phys. **96**, 9060 (1992).
[39] M. Parrinello and A. Rahman, Phys. Rev. Lett. **45**, 1196 (1980).
[40] S. Yashonath and C. N. R. Rao, Mol. Phys. **54**, 245 (1985).
[41] G. S. Dubey, S. O'Shea, and P. A. Monson, Mol. Phys. **80**, 997 (1993).
[42] R. Agrawal and D. A. Kofke, Mol. Phys. **85**, 43 (1995).
[43] A. R. Shultz and P. J. Flory, J. Am. Chem. Soc. **74**, 4760 (1952).
[44] P. J. Flory, *Principles of Polymer Chemistry* (Cornell University Press, Ithaca, 1954).
[45] M. G. Broadhurst, J. Res. Natl. Bur. Stand., Sect. A **66A**, 241 (1962).
[46] J. C. Pamies and L. F. Vega, Ind. Eng. Chem. Res. **40**, 2532 (2001).
[47] Y. J. Sheng, A. Z. Panagiotopoulos, and S. K. Kumar, Macromolecules **27**, 400 (1994).
[48] E. P. A. Paras, C. Vega, and P. A. Monson, Mol. Phys. **79**, 1063 (1993).
[49] C. Vega, B. Garzon, S. Lago, and P. A. Monson, J. Mol. Liq. **76**, 157 (1998).
[50] D. A. McQuarrie and J. D. Simon, *Physical Chemistry: A Molecular Approach* (University Science Books, Sausalito, 1997).
[51] D. L. Morgan and R. Kobayashi, Fluid Phase Equilib. **63**, 317 (1991).
[52] E. D. Nikitin, High Temp. **36**, 305 (1998).
[53] J. P. Ryckaert and A. Bellemans, Faraday Discuss. Chem. Soc. **66**, 95 (1978).
[54] A. Lopez Rodriguez, C. Vega, J. J. Freire, and S. Lago, Mol. Phys. **80**, 1565 (1993).
[55] B. Smit, S. Karaborni, and J. I. Siepmann, J. Chem. Phys. **102**, 2126 (1995); **109**, 352(E) (1998).
[56] A. Lopez Rodriguez, C. Vega, and J. J. Freire, J. Chem. Phys. **111**, 438 (1999).